https://doi.org/10.17221/140/2022-SWR

Influence of *Paulownia fortunei* (Seem.) Hemsl. roots on preferential flow in the red soil hilly region

Zhuo Tian[1,2], Shuaipu Zhang[1,2], Qinxue Xu[1,2], Mingfeng Bi[1,2], Jianhua He[1,2]*

[1]*Guangxi Key Laboratory of Environmental Pollution Control Theory and Technology, Guilin University of Technology, Guilin, Guangxi, P.R. of China*
[2]*Collaborative Innovation Center for Water Pollution Control and Water Safety in Karst Area, Guilin University of Technology, Guilin, Guangxi, P.R. of China*

**Corresponding author: shuaipuzhang@glut.edu.cn*

Citation: Tian Z., Zhang S.P., Xu Q.X., Bi M.F., He J.H. (2023): Influence of *Paulownia fortunei* (Seem.) Hemsl. roots on preferential flow in the red soil hilly region. Soil & Water Res., 18: 89–101.

Abstract: Preferential water flow in soil significantly affects runoff, water infiltration, storage, groundwater environment, and soil stability. Plant roots positively affect preferential flow development. This study explored the relationship between the root system of *Paulownia fortunei* (Seem.) Hemsl. and preferential flow using dyeing tracer test and image analysis techniques. A typical red soil hilly region on the outskirts of Guilin City (Guangxi, China) was selected as the study area. A Bright Blue solution was used to visualize the pathways followed by the infiltrated water in simulated rainfall experiments, and Image Analyzer of Plants was used to analyze the root length, surface area, and volume. The results revealed significant differences in the root surface area density of coarse roots (RSAD-CR) and length index of preferential flow (LI) among soil profiles at various distances from the tree trunk. The root volume density of coarse (RVD-CR) and total roots (RVD-TR), the root length density of coarse roots (RLD-CR), and RSAD-CR were significantly correlated with the characteristics of dyeing morphology. Conversely, the root length density and root surface area density of fine (RLD-FR and RSAD-FR, respectively) and total roots (RLD-TR and RSAD-TR, respectively), and the root volume density of fine roots (RVD-FR) were not significantly correlated with the characteristic parameters of dyeing morphology. The root systems of *P. fortunei* were critical for enhancing soil water infiltration and developing preferential flow in red soil hilly regions. Coarse roots had a greater impact on the development of preferential flow than fine roots, and root volume had a greater influence on preferential flow development than root length and root surface area. This study contributes to a better understanding of the hydrological cycle at the plant-soil interface in red soil hilly regions.

Keywords: dyeing experiment; principal component analysis (PCA); root distribution; water infiltration

Soil water is a vital part of terrestrial ecosystems, combining the interactions between soil, plants, and climate (Wang et al. 2019; Yu et al. 2001; Rodriguez-Iturbe 2003). As a result of frequent seasonal droughts in the red soil hilly areas of South China, the reduction in soil moisture can promote the formation of dry soil horizons, which endangers vegetation sustainability (Jia et al. 2017, 2019; Guo et al. 2019). Water infiltration plays a vital role in water accessibility in the soil and is thus crucial to ecological conservation (Wang et al. 2007, 2019).

As a major form of water infiltration, preferential flow is considered a typical process of moving water through unsaturated soils (Wang & Zhang

Supported by the National Natural Science Foundation of China, Project No. 41907011, and by the Natural Science Foundation of Guangxi, Project No. 2018GXNSFBA050013.

https://doi.org/10.17221/140/2022-SWR

2011; Nimmo 2012; Sheng et al. 2014; Zhang et al. 2016). Preferential flow allows water to move quickly to deeper soils by circumventing a major portion of the soil matrix and contributing 11~54% of the total solutes transferred by water flow (Legout et al. 2009; van der Heijden et al. 2013; Laine-Kaulio et al. 2014; Luo et al. 2019b). Previous studies have demonstrated that preferential flow ameliorates land degradation by increasing soil infiltration, regulating runoff, and reducing soil erosion (Allaire et al. 2011; Mei et al. 2018; Dai et al. 2022). However, preferential flow is unpredictable because of its random spatial and temporal distribution in the soil (Pruess 1998; Zhang et al. 2015, 2017; Guo et al. 2019). Therefore, understanding preferential flow infiltration is vital for the use and management of surface and groundwater resources.

Many factors influence the formation, distribution, and differentiation of preferential flows (Cheng et al. 2011). These include soil type and structure, biological activities (earthworms and root channels), soil water content, and hydraulic conditions (Hardie et al. 2011; Vannoppen et al. 2015; Yi et al. 2019). For the past few years, the response of preferential flow to the plant root system, as well as soil water movement, has been an active area in pedological and hydrological research (Zhang et al. 2017). The soil moisture movement and plant growth have a mutual feed relationship (Wang et al. 2019; Wu et al. 2021). Soil moisture infiltration affects plant growth, and plant roots form continuous preferential channels (Tracy et al. 2011). The rhizosphere increases the organic matter content in the root zone, supports the aggregation of the soil (Fageria & Stone 2006), and improves the overall stability of the soil, thereby extending the long life of the channels (Ghestem et al. 2011). Decayed roots may also form long, continuous, preferential channels that encourage the downflow of water (Jiang et al. 2018; Guo et al. 2019; Nespoulous et al. 2019).

Although many studies have shown that plant roots have important effects on preferential flow development, the influence of coarse and fine living roots on preferential flow is not clear. In this study, the indices of root system characteristics and characteristic parameters of the dyeing morphology were calculated. The root system characteristic indices include the root length density of coarse (RLD-CR), fine (RLD-FR), and total roots (RLD-TR), root surface area density of coarse (RSAD-CR), fine (RSAD-FR), and total roots (RSAD-TR), and the root volume density of coarse (RVD-CR), fine (RVD-FR), and total roots (RVD-TR). The characteristic parameters of dyeing morphology include the depth of uniform flow (UF), dye coverage (DC), preferential flow fraction (PF), length index (LI), maximum dyed depth (MD), variation coefficient of dye coverage (CV), depth of the dye coverage at the 50% level (0.5DC), and the maximum depth of the dyed area to the depth of dye coverage at the 50% level (MD/0.5DC). This study aims to: (1) evaluate the effect of fine and coarse roots in *Paulownia fortunei* (Seem.) Hemsl. on preferential flow development, and (2) quantitatively determine the correlation between the root system characteristic indices and the characteristic parameters of dyeing morphology using principal component analysis (PCA).

MATERIAL AND METHODS

Study sites. This study was conducted on the outskirts of Guilin City, Guangxi, China (110°14'46''~110°29'14''E, 24°59'51''~25°14'17''N; Figure 1). The study area is typical of the red soil hilly region, which is climatically characterized as a mild subtropical monsoon area with sufficient light. The annual average temperature is 19.2 °C. The peak temperature occurs between June and September every year, and the lowest temperature occurs between January and February. The annual average rainfall is 1903 mm, with a monthly maximum of 359 mm in June and a monthly minimum of 50 mm in October. The uneven distribution of rainfall events leads to frequent seasonal droughts.

The slope of the study site was approximately 22°, with an altitude of 175~185 m. The vegetation was dominated by *Paulownia fortunei* (Seem.) Hemsl., *Miscanthus sinensis* Anderss., *Setaria viridis* (Linn.) Beauv., and *Polygonum perfoliatum* L. The soil texture at the study site was loam clay or sandy clay loam. The basic physical properties of the examined soils are listed in Table 1.

Dyeing experiment. Three field research areas (5 × 5 m) were selected on the slope, and within each area, one *P. fortunei* plant was planted. These were allowed to grow for one year before experimental work was started. The growth trends of the plants were comparable, as shown in Table 2.

A 0.6 × 0.6 m quadrat was delineated around the plant in each area. Within these quadrats, the litter layer was carefully removed to expose the soil surface (Guo et al. 2019). Later, stainless steel

https://doi.org/10.17221/140/2022-SWR

Table 1. Basic soil physical properties in the study site

Soil depth (cm)	Bulk density (g/cm^3)	Soil porosity (%)	Specific surface area of soil particles ($10^4 \cdot cm^2/cm^3$)	Mechanical composition (%)			Saturation water content (%)	Field capacity (%)
				clay content (0~2 μm)	silt content (2~20 μm)	sand content (20~2 000 μm)		
0–10	1.61 ± 0.04^{c}	39.41 ± 1.47^{a}	2128.00 ± 80.78^{b}	19.73 ± 1.28^{b}	17.52 ± 1.40^{b}	62.76 ± 2.66^{a}	22.39 ± 1.08^{a}	18.27 ± 0.75^{a}
10–20	1.58 ± 0.01^{c}	40.39 ± 0.31^{a}	5922.00 ± 1070.25^{a}	37.71 ± 4.52^{a}	19.23 ± 2.09^{ab}	43.07 ± 6.57^{b}	21.64 ± 0.33^{ab}	15.44 ± 1.92^{ab}
20–30	1.78 ± 0.03^{a}	32.97 ± 1.10^{c}	4794.33 ± 196.41^{a}	33.35 ± 1.91^{a}	26.10 ± 1.38^{a}	40.56 ± 3.29^{b}	16.26 ± 0.57^{c}	12.14 ± 1.07^{b}
30–40	1.72 ± 0.05^{ab}	34.91 ± 2.04^{bc}	4633.33 ± 699.79^{a}	30.67 ± 3.46^{ab}	23.14 ± 2.14^{ab}	46.19 ± 5.44^{ab}	18.56 ± 2.20^{bc}	15.26 ± 2.49^{ab}
40–50	1.69 ± 0.02^{b}	36.35 ± 0.83^{b}	4577.00 ± 1379.72^{a}	33.97 ± 9.59^{a}	25.60 ± 5.67^{a}	40.42 ± 15.07^{b}	19.89 ± 1.83^{ab}	16.90 ± 2.12^{a}

Specific surface area of soil particles and mechanical composition of soil samples were measured using a laser particle size analyzer (Mastersizer 3000, Great Malvern, UK); soil porosity, bulk density, saturation water content, and field capacity were measured using the ring knife method; the presented values are mean ± standard deviation; different lowercase letters in the same column indicate significant differences among various soil layers ($P < 0.05$)

plates (0.3 m in height) were placed in a concentric manner on the surface of the soil and then gently inserted 0.1 m vertically into the soil to minimize the possibility of crack formation. Moreover, the soil was carefully compacted within 5 cm of the frame to prevent the applied dye from infiltrating along the quadrat frame (Yao et al. 2017). Each quadrat was covered with a high-density polyethylene plastic film for 24 h to ensure that all quadrats had a similar soil water content at the start of the dyeing experiment.

A Bright Blue solution (4 g/L) was selected to illustrate the non-uniform distribution of flow in the soil (Lipsius & Mooney 2006; Allaire et al. 2009). There was no rainfall for three days before the experiment. To achieve a reliable dyeing result (based on the results of a preliminary experiment), 27 L of Bright Blue solution was sprayed uniformly onto the three 0.6 × 0.6 m areas. The spraying process lasted for 3 h. Each quadrat was covered with plastic film to prevent evaporation of the applied solution. The film was removed 24 h after infiltration had stopped (Mei et al. 2018).

To avoid the cutting process from impacting the soil structure, for each plate, a 5 cm buffer zone was left at the inner circle. The final data for each treatment were collected in a 0.5 × 0.5 m stained area in the centre of the quadrat, in which the quadrats were cut into five slices vertically with 10 cm spaces between them (Kan et al. 2020), as shown in Figure 2. Calibrated frames were designed inside the soil profile to assist with the subsequent image correction process (Jiang et al. 2017). In cases of high sunlight intensity, an umbrella was used to decrease shadow interference (Hagedorn & Bundt 2002). Using a 13-megapixel camera, each vertical profile was photographed and 18 stained profile images were obtained.

Image processing and data analysis. Images were post-processed using Photoshop CS3 (Adobe Systems Inc., San Jose, CA, USA) and Image Pro Plus software (Ver. 6.0; Media Cybernetics Inc., Rockville, USA) to quantify the areas marked as stained (Yao et al. 2017). The captured images were geometrically corrected using Photoshop CS3. For size modification, the vertical sections of the image were then modified by cropping to 0.5 × 0.5 m using the image ruler function. The features of the pictures, such as saturation, image brightness, grayscale, and image threshold value, were later modified to the desired values and percentages. The captured images were then digitized using Image Pro Plus (Ver. 6.0). For each image, the

https://doi.org/10.17221/140/2022-SWR

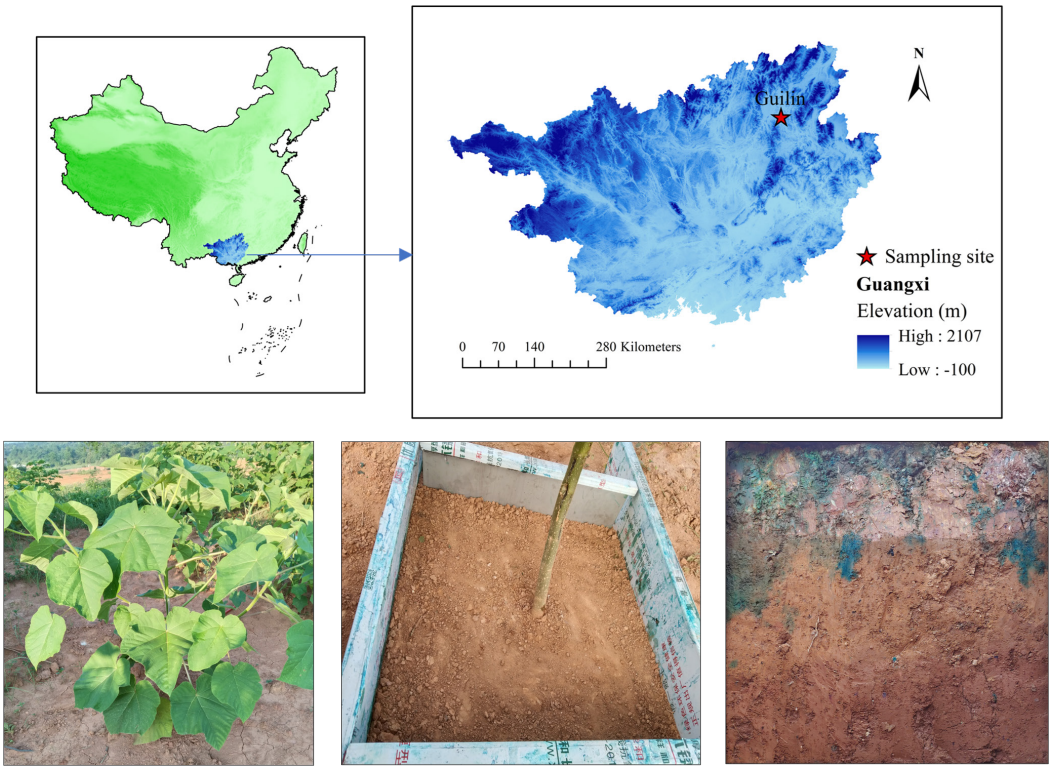

Figure 1. Location of the experimental site in the Guangxi Zhuang Autonomous Region, China

pixels were set at 500 × 500 for conversion of the image into binary information and classified into black (where a pixel value of 0 represents dyed areas) and white (where a pixel value of 255 represents undyed areas), as shown in Figure 3. The corresponding characteristic parameters of dyeing morphology were calculated using Image Pro Plus (Ver. 6.0) to convert binary information into a binary data matrix.

The dye coverage (DC) indicates the percentage of areas that were dyed (Flury & Fluhler 1994; Liu et al. 2021), and is calculated using the following formula:

$$DC = \frac{D}{D + ND} \times 100\% \quad (1)$$

where:
DC – the dye coverage (%) in the soil profile;
D – the stained areas (cm^2);
ND – the unstained areas (cm^2).

The depth of uniform flow (UF) refers to the depth at which the coverage of the dye reduces to less than 80%. Therefore, soils with a higher degree of preferential flow will have lower values of such an index (Tobella et al. 2014).

The preferential flow fraction (PF) is an indicator that is normally applied to show the distribution and degree of preferential flow (Sollins & Radulovich 1988; van Schaik 2009) and is obtained using the following formula:

$$PF = \left(1 - \frac{UF \times W}{DT}\right) \times 100\% \quad (2)$$

where:
PF – the soil preferential flow fraction (%);
W – the width of the horizontal soil profile (cm);
UF – the uniform flow depth (the matrix flow) (cm);
DT – the total dyed portion of the soil in cm^2.

Table 2. Growth parameters of *Paulownia fortunei* over one year (in cm)

Plant	Plant height	East-west canopy	South-north canopy	Ground diameter
1	138.46	149.72	154.11	2.81
2	139.23	170.25	162.31	2.79
3	135.94	164.13	161.52	2.76

The ground diameter was measured at 20 cm above the ground

https://doi.org/10.17221/140/2022-SWR

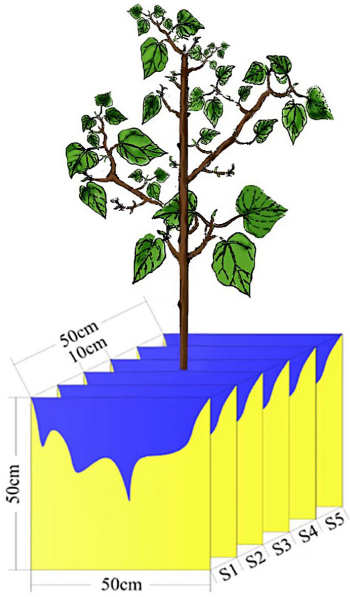

Figure 2. Schematic diagram of soil staining experiment
S1 to S5 represents five different soil profiles at various distances from the tree trunk

The preferential flow length index (LI) is positively correlated with the degree of heterogeneity of preferential flow (Tobella et al. 2014). LI is calculated as:

$$LI = \sum_{i=1}^{n} \left| DC_{(i+1)} - DC_i \right| \quad (3)$$

where:

LI – the preferential flow length index (%);

n – the total number of pixels of the soil section in its vertical profile (equal to 500 for the current work);

DC_i – the dyeing area ratio to the i^{th} layer in %.

The variation coefficient of dye coverage (CV) is applied to quantitatively explain changes in the morphology of applied dyeing and is calculated as (Kan et al. 2019):

$$CV = \frac{\sqrt{\frac{1}{N-1}\sum_{i=1}^{N}\left(DC_i - \overline{DC}\right)^2}}{\frac{1}{N}\sum_{i=1}^{N} DC_i} \quad (4)$$

where:

CV – the variation coefficient of DC in the preferential flow zone;

N – the number of soil sections for preferential flow in the vertical profile (500 in this study);

$\overline{DC}$ – the average staining area ratio value;

DC_i – the dye area ratio of the soil profile in the i^{th} layer.

The maximum dyed depth (MD) refers to the deepest penetration of water in the preferential flow paths and describes the characteristics of the rapid infiltration of preferential flow (van Schaik 2009). A depth of 50% dye coverage (0.5DC) represents the infiltration depth of water when the dye area ratio is 50%. The larger the MD/0.5DC, the more prominent the preferential flow occurrence in the deeper horizons (Xie et al. 2021).

Root measurement and data analysis. Roots were collected when the soil profiles were excavated. Soil blocks containing roots were transported to the laboratory, and roots were removed, cleaned, dried, and scanned using a flatbed scanner (Hao et al. 2021). Root length, surface area, and volume were analyzed using LA-S software (Multifunctional Image Analyzer of Plants, Wseen Ltd., Hangzhou, China) (Hao et al. 2020). Roots were classified into two diameter categories (fine, ≤ 2 mm; coarse, > 2 mm) (Stokes et al. 2009; Nespoulous et al. 2019). Root length density (RLD), root volume density (RVD), and root surface area density (RSAD) were calculated as (Ning et al. 2019):

$$RLD = \frac{RL}{SV} \quad (5)$$

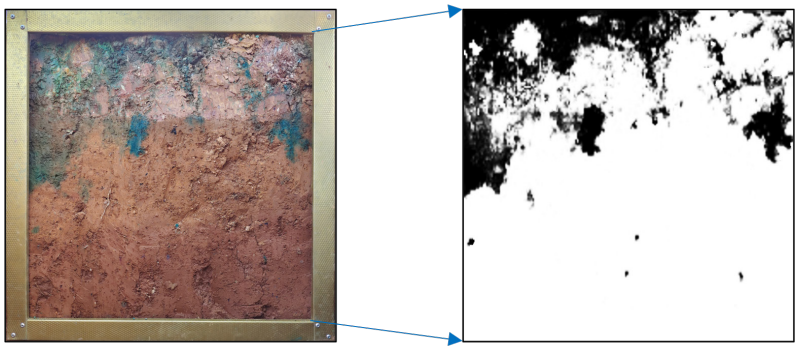

Figure 3. Image treatment of the dyed soil profile

https://doi.org/10.17221/140/2022-SWR

$$RVD = \frac{RV}{SV} \quad (6)$$

$$RSAD = \frac{RSA}{SV} \quad (7)$$

$$RV = RL \times \frac{1}{4} \pi d^2 \quad (8)$$

$$RSA = RL \times \pi d \quad (9)$$

where:
RLD – expressed in cm/cm^3;
RVD – expressed in cm^3/cm^3;
RSAD – expressed in cm^2/cm^3;
RL – the root length (cm);
SV – the soil volume (cm^3);
RV – the root volume (cm^3);
RSA – the root surface area (cm^2);
d – the average diameter of the root system (cm).

Statistical analysis. The images were plotted using Origin Pro 2018 software (OriginLab, Northampton, Massachusetts, USA), and statistical analyses were performed using SPSS 22.0 software (IBM Corporation, Armonk, New York, USA). One-way analyses of variance (ANOVA) were applied to determine the differences in the root system characteristic indices and the characteristic parameters of dyeing morphology between each soil profile with a significance of 0.05. Spearman correlation analysis and principal component analysis (PCA) were used to calculate the correlation between the root system characteristic indices and the characteristic parameters of dyeing morphology.

RESULTS

Distribution characteristics of roots. Figure 4 shows the differences in the distribution characteristics of the total, fine, and coarse roots. Overall, the RLD in S1 was the largest among all the profiles. The RVD and RSAD values in S3 were larger than those in the other profiles. There were no significant differences in RLD, RVD, and RSAD between the profiles at various distances from the tree trunk. The RLD, RVD, and RSAD of fine roots in S1 were larger than those in the other profiles, whereas those in S4 were lower than those in the other profiles. No significant differences were found in the RLD,

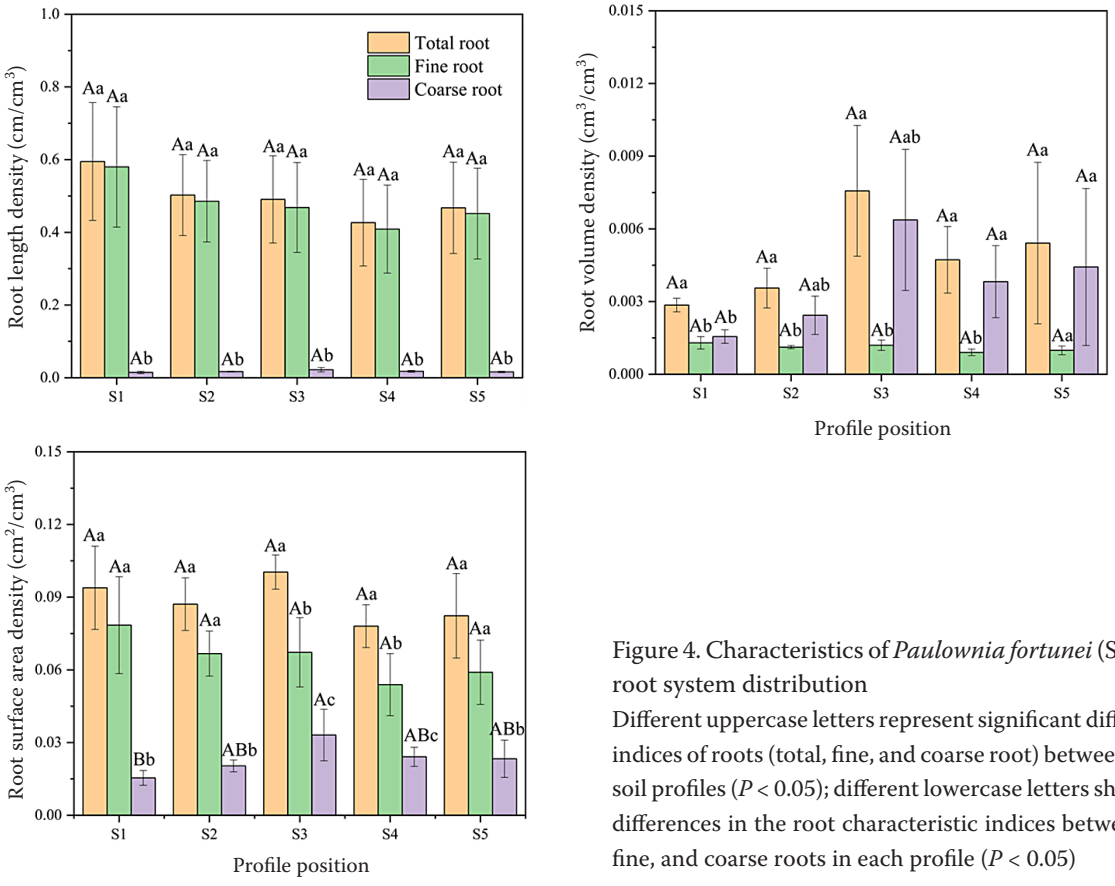

Figure 4. Characteristics of *Paulownia fortunei* (Seem.) Hemsl. root system distribution

Different uppercase letters represent significant differences in the indices of roots (total, fine, and coarse root) between the different soil profiles ($P < 0.05$); different lowercase letters show significant differences in the root characteristic indices between total root, fine, and coarse roots in each profile ($P < 0.05$)

https://doi.org/10.17221/140/2022-SWR

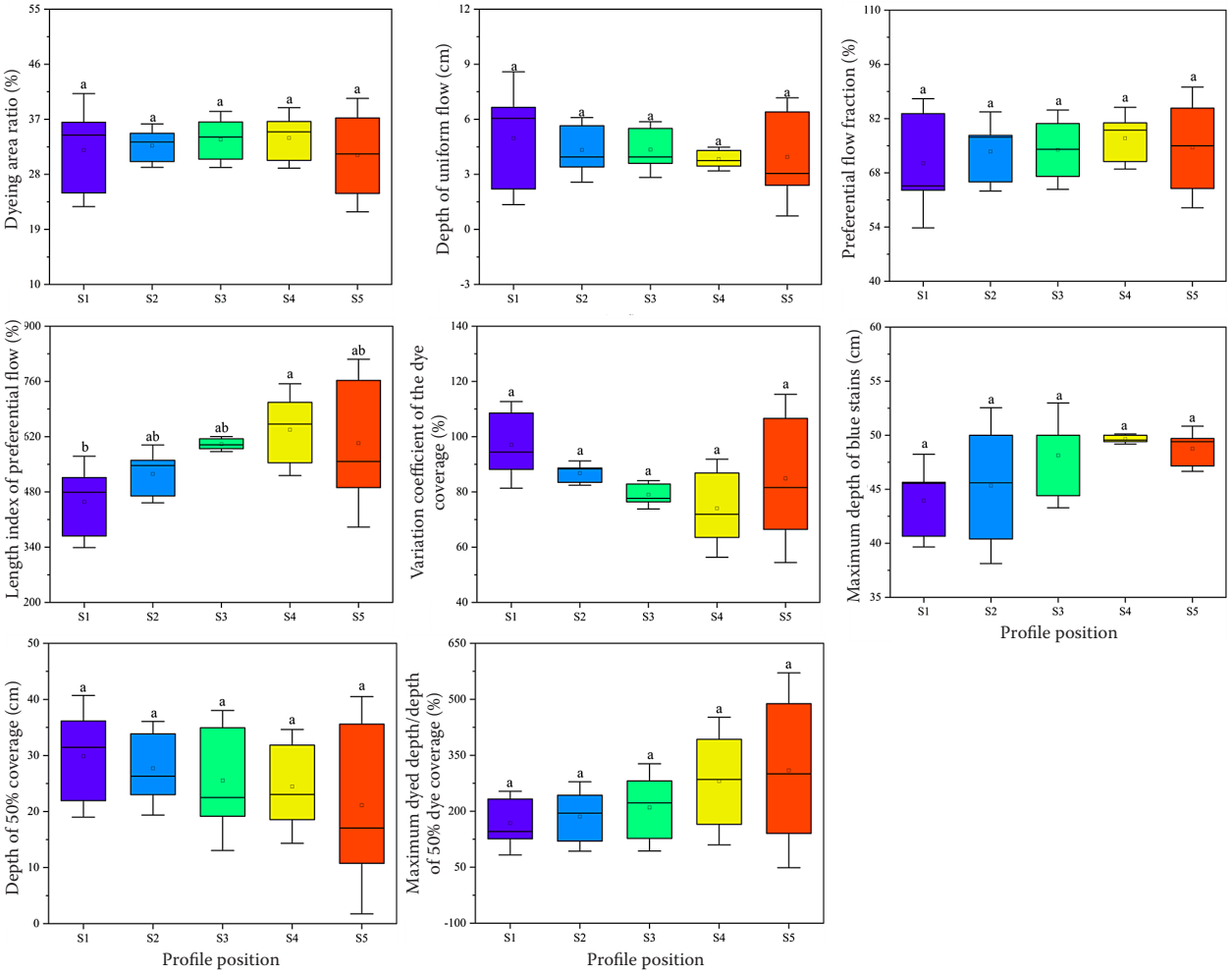

Figure 5. Characteristic parameters of preferential flow

Different lowercase letters indicate significant differences in the characteristic parameters of preferential flow between different soil profiles ($P < 0.05$)

RVD, and RSAD of the fine roots between the different profiles at various distances from the tree trunk. The RLD, RVD, and RSAD of coarse roots in S3 were higher than those in the other profiles, whereas those in S1 were lower than those in the other profiles. No significant differences were observed in the RLD and RVD of coarse roots between the profiles at various distances from the tree trunk. The RSAD of coarse roots in the profile where the trunk was located (S3) was significantly larger than that in the profile farthest from the trunk (S1).

Preferential flow development characteristics. Figure 5 shows the differences in the characteristic parameters of the dyeing morphology of the soil profiles at various distances from the tree trunk. The DC, PF, LI, and MD values in S4 were larger than those in the other profiles. DC was lower in S5 than in the other profiles. The PF, LI, and MD values of S1 were lower than those of the other profiles. UF and CV were the largest in S1 and the smallest in S4. The 0.5DC was the largest in S1 and the smallest in S5, whereas the opposite was true for MD/0.5DC. The LI differed significantly between S1 and S4 but not between the other soil profiles. There were no significant differences in the DC, UF, PF, CV, MD, 0.5DC, and MD/0.5DC between the profiles at various distances from the tree trunk.

Relationships between root and preferential flow. Table 3 shows that the RSAD-CR was significantly negatively correlated with UF. The RLD-CR and RSAD-CR were significantly positively correlated with the PF. The RVD-TR and RVD-CR were highly significantly positively correlated with the LI. The RSAD-CR had a significant positive correlation with

https://doi.org/10.17221/140/2022-SWR

Table 3. Spearman correlation matrix of characteristic parameters of dyeing morphology and root system characteristic indexes

Index	RLD-TR	RSAD-TR	RVD-TR	RLD-FR	RLD-CR	RSAD-FR	RSAD-CR	RVD-FR	RVD-CR
DC	−0.371	−0.289	−0.032	−0.379	−0.089	−0.246	−0.086	−0.221	0
UF	0.281	0.223	−0.366	0.265	−0.492	0.395	−0.517*	0.418	−0.408
PF	−0.371	−0.257	0.482	−0.364	0.575*	−0.475	0.621*	−0.493	0.493
LI	−0.311	0.021	0.689**	−0.346	0.407	−0.271	0.639*	−0.239	0.707**
MD	0.229	0.344	0.404	0.198	−0.029	0.195	0.269	0.119	0.435
CV	0.332	−0.018	−0.714**	0.346	−0.368	0.314	−0.643**	0.364	−0.729**
0.5DC	−0.268	−0.321	−0.407	−0.257	−0.221	−0.111	−0.379	−0.057	−0.389
MD/0.5DC	0.007	0.089	0.486	0.004	0.243	−0.125	0.489	−0.207	0.518*

DC – dye coverage; UF – depth of uniform flow; PF – preferential flow fraction; LI – length index; MD – maximum dyed depth; CV – variation coefficient of dye coverage; 0.5DC – depth of dye coverage at 50% level; MD/0.5DC – maximum depth of the dyed area to the depth of 50% dye coverage; RLD – root length density; RSAD – root surface area density; RVD – root volume density; TR – total root; FR – fine root; CR – coarse root; **, *significant correlations at $P < 0.01$ and 0.05, respectively

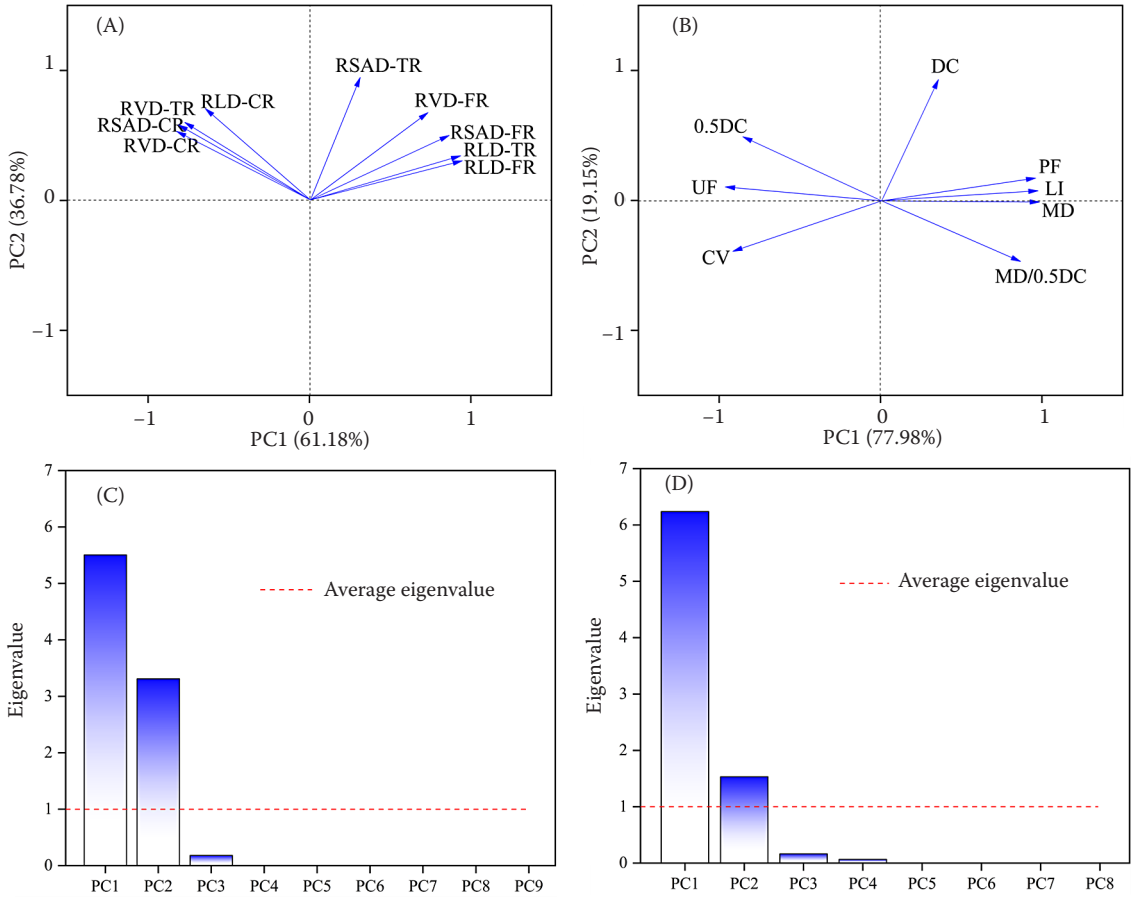

Figure 6. Principal component analysis of the root system characteristics indexes (A, C) and the characteristic parameters of dyeing morphology (B, D)

DC – dye coverage; UF – depth of uniform flow; PF – preferential flow fraction; LI – length index; MD – maximum dyed depth; CV – variation coefficient of dye coverage; 0.5DC – depth of dye coverage at 50% level; MD/0.5DC – maximum depth of the dyed area to the depth of 50% dye coverage; RLD – root length density; RSAD – root surface area density; RVD – root volume density; TR – total root; FR – fine root; CR – coarse root

https://doi.org/10.17221/140/2022-SWR

Table 4. Principal component score of root and preferential flow

Profile position	Root			Preferential flow		
	PC 1	PC 2	final score	PC 1	PC 2	final score
S1	3.728	0.279	2.433	–3.673	–0.207	–2.989
S2	0.846	–0.593	0.306	–1.172	0.387	–0.864
S3	–1.622	2.990	0.109	0.569	0.994	0.653
S4	–1.943	–1.722	–1.860	2.696	0.872	2.336
S5	–1.009	–0.954	–0.988	1.579	–2.046	0.865

the LI. The RVD-TR, RVD-CR, and RSAD-CR were highly significantly negatively correlated with the CV. The RVD-CR was also significantly positively correlated with MD/0.5DC. The RLD-TR, RSAD-TR, and all indices of fine roots were not significantly correlated with any characteristic parameters of dyeing morphology.

The outcomes of PCA revealed that the cumulative interpretation variance ratios of the first two axes were 97.96% (the root system characteristic indices) and 97.13% (the characteristic parameters of dyeing morphology) (Figure 6). For the root system characteristic indices RSAD-TR, RLD-TR, and all indexes of fine roots were concentrated on the positive semi-axis of PC 1, whereas the opposite was found for RVD-TR and all indexes of coarse roots (Figure 6A). For the characteristic parameters of dyeing morphology, 0.5DC, UF, and CV were concentrated on the negative semi-axis of the PC 1, whereas the opposite was found for the DC, PF, LI, MD, and MD/0.5DC (Figure 6B).

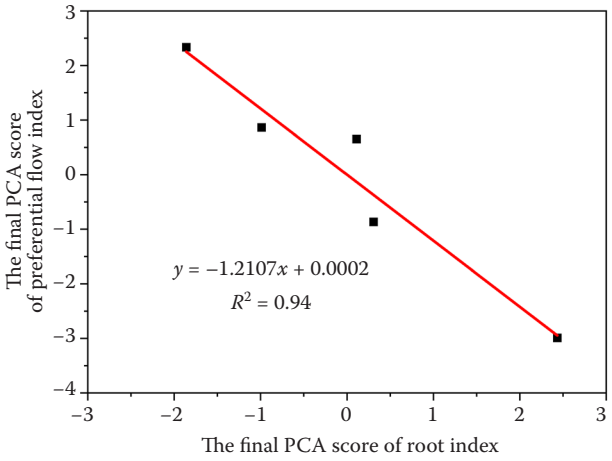

Figure 7. Relationship of the final principal component analysis (PCA) scores between root index and preferential flow index

The first two PCA axes were extracted to calculate the principal component scores (Table 4). The final scores were most affected by PC 1 because the interpretation variance ratios of PC 1 were 61.18% (the root system characteristics indexes) and 77.98% (the characteristic parameters of dyeing morphology) (Figure 6). There was a strong negative relationship (with $R^2 = 0.94$) between the root system characteristic indices and the characteristic parameters of dyeing morphology (Figure 7), indicating that the larger the RVD-TR, RVD-CR, RSAD-CR, and RLD-CR, the stronger the development of preferential flow. From the above results, it can be concluded that coarse roots had a greater effect than fine roots on preferential flow development, and root volume had a greater effect than root length and root surface area on preferential flow development.

DISCUSSION

Soil water infiltration is closely associated with plant water storage, root morphology, soil physical properties, soil erosion, surface runoff, and groundwater recharge (Lipiec et al. 2006; Jiang et al. 2018; Guo et al. 2019). The two major types of water infiltration into the soil are matrix and preferential flows (Ghestem et al. 2011; Zhang et al. 2016). The former exists in an unsaturated environment and is influenced by capillary suction (Zhang et al. 2017). Preferential flow is usually in the vertical direction and is due mainly to gravitational potential (Germann et al. 2007). Preferential flow is generated by many factors, including non-homogeneous infiltration, macropore flow, lateral flow, and instabilities of the wetting front (Bundt et al. 2001; Allaire et al. 2009), which are difficult to describe using existing theories (Vries & Chow 1978; Weiler 2005). In this study, most of the dye settled in the upper soil layer. This phenomenon indicates that the preferential

https://doi.org/10.17221/140/2022-SWR

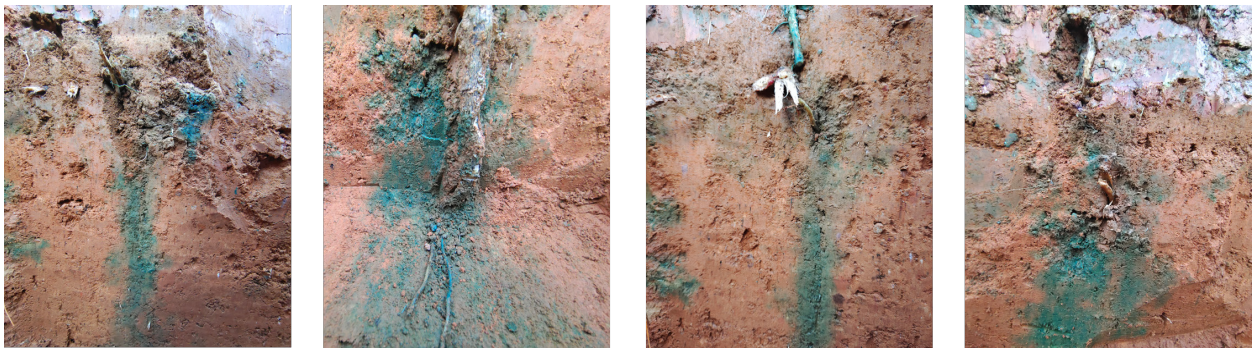

Figure 8. Pictures of independent stained patches with coarse roots

and matrix flows interact with each other and have high hydrological connectivity in the upper soils. In addition, these outcomes were aligned with the reported results of Guo et al. (2019) and Devitt and Smith (2002). Previous research has shown that the dye coverage in the upper horizons of the soil was more extensive than that in the deeper horizons because preferential flow was more frequent in the upper horizons of the soil profile than that in the deeper horizons (Zhang et al. 2015).

Plant roots have important impacts on soil structure and moisture and further affect the development of preferential flow (Luo et al. 2019a; Wu et al. 2021). Several studies have shown that water discharges from visibly dead root channels; however, water has also been found to flow through living root channels (Noguchi et al. 1997; Newman et al. 2004). Different channel types linked to roots can function as pathways for preferential flow and interact to form a network (Sidle et al. 2001). This study showed that the UF was smaller than 10 cm in all soil profiles, and there was evident morphological differentiation of staining in the 0 ~ 10 cm soil layer. This result may be associated with the distribution of roots in the upper layers of the soil (Gale & Grigal 1987). Roots affect water infiltration mainly by increasing soil porosity because roots evolve in the soil, leaving annular or semi-annular spaces for possible water flows as root diameter changes (Ghestem et al. 2011). In addition, the volume of the root retracts during the dry season (Nobel & Cui 1992). Under the action of wind, trunk flexing causes the roots and soil around the root channel to move slightly, and pores are formed between the living roots and the root channel (Ghestem et al. 2011).

Root size and rooting depth can affect soil water infiltration and redistribution (Archer et al. 2002; Leung et al. 2015). Root structures with very thick and shallow roots well connected to the plant stems might enhance lateral subsurface flow, whereas root structures with thinner lateral roots and thicker vertical taproots would facilitate vertical water flow (Ghestem et al. 2011). This study showed that none of the indices of fine roots significantly correlated with any of the characteristic parameters of dyeing morphology, whereas several indices of coarse roots significantly correlated with characteristic parameters of dyeing morphology. These results are consistent with those observed in the field experiments. Independent staining patches were typically accompanied by coarse roots in the soil profile (Figure 8). These results concur with the conclusions of Devitt and Smith (2002), who illustrated that the water percolation via root channels improved with the growing measurement of the root systems. The results of the PCA showed that preferential flow development was closely correlated with the roots. Coarse roots had a greater effect on preferential flow development than fine roots. This outcome was inconsistent with the results reported by Luo et al. (Luo et al. 2019b), who demonstrated that coarse roots contributed less to preferential water transport than fine roots because fine roots made up a much larger proportion of the total root occurrence of the soil profile. The PCA also indicated that root volume had a greater effect on preferential flow development than root length and surface area. Coarse roots can amplify the radius of the root channels via the physical action of the root and improve water infiltration (Ghestem et al. 2011; Bodner et al. 2014). The thicker the root, the larger the root volume. Hence, root volume contributed more to preferential flow development than root length and surface area.

https://doi.org/10.17221/140/2022-SWR

CONCLUSION

This study analysed the relationships between root system characteristic indices of *P. fortunei* and the characteristic parameters of the dyeing morphology. The results of this study indicated that distance from the tree trunk (as measured in this study) did not appear to have any significant effect on root system characteristics or characteristic parameters of dyeing morphology except for the density of the root surface area of coarse roots and length index of preferential flow. There was a strong relationship between the root system characteristic indices and the characteristic parameters of the dyeing morphology. The root systems of *P. fortunei* were critical for enhancing soil water infiltration and developing the preferred flow in red soil hilly regions. The coarse roots had a larger impact on preferential flow development than the fine roots, and the root volume had a larger influence on preferential flow development than the root length and root surface area.

REFERENCES

Allaire S.E., Roulier S., Cessna A.J. (2009): Quantifying preferential flow in soils: A review of different techniques. Journal of Hydrology, 378: 179–204.

Allaire S.E., Van bochove E., Denault J.T., Dadfar H., Theriault G., Charles A., De jong R. (2011): Preferential pathways of phosphorus movement from agricultural land to water bodies in the Canadian Great Lakes basin: A predictive tool. Canadian Journal of Soil Science, 91: 361–374.

Archer N.A.L., Quinton J.N., Hess T.M. (2002): Below-ground relationships of soil texture, roots and hydraulic conductivity in two-phase mosaic vegetation in South-east Spain. Journal of Arid Environments, 52: 535–553.

Bodner G., Leitner D., Kaul H.P. (2014): Coarse and fine root plants affect pore size distributions differently. Plant and Soil, 380: 133–151.

Bundt M., Widmer F., Pesaro M., Zeyer J., Blaser P. (2001): Preferential flow paths: Biological 'hot spots' in soils. Soil Biology & Biochemistry, 33: 729–738.

Cheng J.H., Zhang H.J., Wang W., Zhang Y.Y., Chen Y.Z. (2011): Changes in preferential flow path distribution and its affecting factors in Southwest China. Soil Science, 176: 652–660.

Dai J.D., Zhang J.H., Xue K., Yang F., Huang F.C., Zhao H., Ma X.Y., Dai C.J., Xu Y.M., Li M.T., Xu H.C. (2022): Effects of spatial variations in rock fragments related to tillage on hydrological processes and sediment transport. Catena, 211: 105963.

Devitt D.A., Smith S.D. (2002): Root channel macropores enhance downward movement of water in a Mojave Desert ecosystem. Journal of Arid Environments, 50: 99–108.

Fageria N.K., Stone L.F. (2006): Physical, chemical, and biological changes in the rhizosphere and nutrient availability. Journal of Plant Nutrition, 29: 1327–1356.

Flury M., Fluhler H. (1994): Brilliant Blue FCF as a dye tracer for solute transport studies: A toxicological overview. Journal of Environmental Quality, 23: 1108–1112.

Gale M.R., Grigal D.F. (1987): Vertical root distribution of northern tree species in relation to successional status. Canadian Journal of Forest Research, 17: 829–834.

Germann P., Helbling A., Vadilonga T. (2007): Rivulet approach to rates of preferential infiltration. Vadose Zone Journal, 6: 207–220.

Ghestem M., Sidle R.C., Stokes A. (2011): The influence of plant root systems on subsurface flow: Implications for slope stability. Bioscience, 61: 869–879.

Guo L., Liu Y., Wu G.L., Huang Z., Cui Z., Cheng Z., Zhang R.Q., Tian F.P., He H.H. (2019): Preferential water flow: Influence of alfalfa (*Medicago sativa* L.) decayed root channels on soil water infiltration. Journal of Hydrology, 578: 124019.

Hagedorn F., Bundt M. (2002): The age of preferential flow paths. Geoderma, 108: 119–132.

Hao H.X., Cheng L., Guo Z.L., Wang L., Shi Z.H. (2020): Plant community characteristics and functional traits as drivers of soil erodibility mitigation along a land degradation gradient. Land Degradation & Development, 31: 1851–1863.

Hao H.X., Qin J.H., Sun Z.X., Guo Z.L., Wang J.G. (2021): Erosion-reducing effects of plant roots during concentrated flow under contrasting textured soils. Catena, 203: 105378.

Hardie M.A., Cotching W.E., Doyle R.B., Holz G., Lisson S., Mattern K. (2011): Effect of antecedent soil moisture on preferential flow in a texture-contrast soil. Journal of Hydrology, 398: 191–201.

Jia X.X., Shao M.A., Zhu Y.J., Luo Y. (2017): Soil moisture decline due to afforestation across the Loess Plateau, China. Journal of Hydrology, 546: 113–122.

Jia X.X., Shao M.A., Yu D.X., Zhang Y., Binley A. (2019): Spatial variations in soil-water carrying capacity of three typical revegetation species on the Loess Plateau, China. Agriculture Ecosystems & Environment, 273: 25–35.

Jiang X.J., Liu S., Zhang H. (2017): Effects of different management practices on vertical soil water flow patterns in the Loess Plateau. Soil & Tillage Research, 166: 33–42.

Jiang X.J., Liu W.J., Chen C.F., Liu J.Q., Yuan Z.Q., Jin B.C., Yu X.Y. (2018): Effects of three morphometric features of roots on soil water flow behavior in three sites in China. Geoderma, 320: 161–171.

https://doi.org/10.17221/140/2022-SWR

Kan X.Q., Cheng J.H., Hu X.J., Zhu F.F., Li M. (2019): Effects of grass and forests and the infiltration amount on preferential flow in karst regions of China. Water, 11: 1634.

Kan X.Q., Cheng J.H., Hou F. (2020): Response of preferential soil flow to different infiltration rates and vegetation types in the karst region of Southwest China. Water, 12: 1778.

Laine-Kaulio H., Backnas S., Karvonen T., Koivusalo H., Mcdonnell J.J. (2014): Lateral subsurface stormflow and solute transport in a forested hillslope: A combined measurement and modeling approach. Water Resources Research, 50: 8159–8178.

Legout A., Legout C., Nys C., Dambrine E. (2009): Preferential flow and slow convective chloride transport through the soil of a forested landscape (Fougeres, France). Geoderma, 151: 179–190.

Leung A.K., Garg A., Coo J.L., Ng C.W.W., Hau B.C.H. (2015): Effects of the roots of Cynodon dactylon and Schefflera heptaphylla on water infiltration rate and soil hydraulic conductivity. Hydrological Processes, 29: 3342–3354.

Lipiec J., Kus J., Slowinska-Jurkiewicz A., Nosalewicz A. (2006): Soil porosity and water infiltration as influenced by tillage methods. Soil & Tillage Research, 89: 210–220.

Lipsius K., Mooney S. J. (2006): Using image analysis of tracer staining to examine the infiltration patterns in a water repellent contaminated sandy soil. Geoderma, 136: 865–875.

Liu Y., Zhang Y.H., Xie L.M., Zhao S.Q., Dai L.Y., Zhang Z.M. (2021): Effect of soil characteristics on preferential flow of Phragmites australis community in Yellow River delta. Ecological Indicators, 125: 107486.

Luo Z.T., Niu J.Z., Xie B.Y., Zhang L., Chen X.W., Berndtsson R., Du J., Ao J.K., Yang L., Zhu S.Y. (2019a): Influence of root distribution on preferential flow in deciduous and coniferous forest soils. Forests, 10: 986.

Luo Z.T., Niu J.Z., Zhang L., Chen X.W., Zhang W., Xie B.Y., Du J., Zhu Z.J., Wu S.S., Li X. (2019b): Roots-enhanced preferential flows in deciduous and coniferous forest soils revealed by dual-tracer experiments. Journal of Environmental Quality, 48: 136–146.

Mei X.M., Zhu Q.K., Ma L., Zhang D., Wang Y., Hao W.J. (2018): Effect of stand origin and slope position on infiltration pattern and preferential flow on a Loess hillslope. Land Degradation & Development, 29: 1353–1365.

Nespoulous J., Merino-Martin L., Monnier Y., Bouchet D.C., Ramel M., Dombey R., Viennois G., Mao Z., Zhang J.L., Cao K.F., Le Bissonnais Y., Sidle R.C., Stokes A. (2019): Tropical forest structure and understorey determine subsurface flow through biopores formed by plant roots. Catena, 181: 104061.

Newman B.D., Wilcox B.P., Graham R.C. (2004): Snowmelt-driven macropore flow and soil saturation in a semiarid forest. Hydrological Processes, 18: 1035–1042.

Nimmo J.R. (2012): Preferential flow occurs in unsaturated conditions. Hydrological Processes, 26: 786–789.

Ning S.R., Chen C., Zhou B.B., Wang Q.Q. (2019): Evaluation of normalized root length density distribution models. Field Crops Research, 242: 107604.

Nobel P.S., Cui M.Y. (1992): Hydraulic conductances of the soil, the root soil air gap, and the root-changes for desert succulents in drying soil. Journal of Experimental Botany, 43: 319–326.

Noguchi S., Nik A.R., Kasran B., Tani M., Sammori T., Morisada K. (1997): Soil physical properties and preferential flow pathways in tropical rain forest, Bukit Tarek, Peninsular Malaysia. Journal of Forest Research, 2: 115–120.

Pruess K. (1998): On water seepage and fast preferential flow in heterogeneous, unsaturated rock fractures. Journal of Contaminant Hydrology, 30: 333–362.

Rodriguez-Iturbe I. (2003): Hydrologic dynamics and ecosystem structure. Water Science and Technology, 47: 18–24.

Sheng F., Liu H.H., Wang K., Zhang R.D., Tang Z.H. (2014): Investigation into preferential flow in natural unsaturated soils with field multiple-tracer infiltration experiments and the active region model. Journal of Hydrology, 508: 137–146.

Sidle R.C., Noguchi S., Tsuboyama Y., Laursen K. (2001): A conceptual model of preferential flow systems in forested hillslopes: Evidence of self-organization. Hydrological Processes, 15: 1675–1692.

Sollins P., Radulovich R. (1988): Effects of soil physical structure on solute transport in a weathered tropical soil. Soil Science Society of America Journal, 52: 1168–1173.

Stokes A., Atger C., Bengough A.G., Fourcaud T., Sidle R.C. (2009): Desirable plant root traits for protecting natural and engineered slopes against landslides. Plant and Soil, 324: 1–30.

Tobella A.B., Reese H., Almaw A., Bayala J., Malmer A., Laudon H., Ilstedt U. (2014): The effect of trees on preferential flow and soil infiltrability in an agroforestry parkland in semiarid Burkina Faso. Water Resources Research, 50: 3342–3354.

Tracy S.R., Black C.R., Roberts J.A., Mooney S.J. (2011): Soil compaction: A review of past and present techniques for investigating effects on root growth. Journal of the Science of Food and Agriculture, 91: 1528–1537.

Van Der Heijden G., Legout A., Pollier B., Brechet C., Ranger J., Dambrine E. (2013): Tracing and modeling preferential flow in a forest soil-potential impact on nutrient leaching. Geoderma, 195: 12–22.

https://doi.org/10.17221/140/2022-SWR

Van Schaik N.L.M.B. (2009): Spatial variability of infiltration patterns related to site characteristics in a semi-arid watershed. Catena, 78: 36–47.

Vannoppen W., Vanmaercke M., De Baets S., Poesen J. (2015): A review of the mechanical effects of plant roots on concentrated flow erosion rates. Earth-Science Reviews, 150: 666–678.

Vries J.D., Chow T.L. (1978): Hydrologic behavior of a forested mountain soil in coastal British Columbia. Water Resources Research, 5: 935–942.

Wang C., Fu B.J., Zhang L., Xu Z.H. (2019): Soil moisture-plant interactions: An ecohydrological review. Journal of Soils and Sediments, 19: 1–9.

Wang K., Zhang R.D. (2011): Heterogeneous soil water flow and macropores described with combined tracers of dye and iodine. Journal of Hydrology, 397: 105–117.

Wang X.P., Li X.R., Xiao H.L., Berndtsson R., Pan Y.X. (2007): Effects of surface characteristics on infiltration patterns in an and shrub desert. Hydrological Processes, 21: 72–79.

Weiler M. (2005): An infiltration model based on flow variability in macropores: development, sensitivity analysis and applications. Journal of Hydrology, 310: 294–315.

Wu Y.N., Zhang Y.H., Xie L.M, Zhao S.Q, Liu Y., Zhang Z.M. (2021): Preferential flow improves root-soil system on a small scale: A case study of two ecotypes of Phragmites communis. Journal of Cleaner Production, 328: 129581.

Xie L.M., Zhang Y.H., Zhang M.X., Zhang Z.M. (2021): Soil preferential flow and nutrient distribution of Robinia pseudoacacia Linn community in Yellow River Delta. Acta Ecologica Sinica, 19: 7713–7724.

Yao J.J., Cheng J.H., Sun L., Zhang X., Zhang H.J. (2017): Effect of antecedent soil water on preferential flow in four soybean plots in Southwestern China. Soil Science, 182: 83–93.

Yi J., Yang Y., Liu M.X., Hu W., Lou S.L., Zhang H.L., Zhang D.Y. (2019): Characterising macropores and preferential flow of mountainous forest soils with contrasting human disturbances. Soil Research, 57: 601–614.

Yu Z.B., Carlson T.N., Barron E.J., Schwartz F.W. (2001): On evaluating the spatial-temporal variation of soil moisture in the Susquehanna River Basin. Water Resources Research, 37: 1313–1326.

Zhang Y.H., Niu J.Z., Yu X.X., Zhu W.L., Du X.Q. (2015): Effects of fine root length density and root biomass on soil preferential flow in forest ecosystems. Forest Systems, 24: e012.

Zhang Y.H., Zhang M.X., Niu J.Z., Zheng H.J. (2016): The preferential flow of soil: A widespread phenomenon in pedological perspectives. Eurasian Soil Science, 49: 661–672.

Zhang Y.H., Niu J.Z., Zhang M.X., Xiao Z.X., Zhu W.L. (2017): Interaction between plant roots and soil water flow in response to preferentlal flow paths in Northern China. Land Degradation & Development, 28: 648–663.

Received: October 16, 2022
Accepted: March 1, 2023
Online first: March 22, 2023